Ionics (2022) 28:3255–3268
https://doi.org/10.1007/s11581-022-04580-w

ORIGINAL PAPER

The structural and ionic conductivity analysis of poly(ethylene oxide)/LiTFSI/MOF-5 nanocomposite electrolytes by using molecular dynamics simulations

Murat Ozlek[1,2] · Engin Burgaz[1,2] · Ibrahim Inanc[1,2] · Muberra Andac[2,3]

Received: 21 March 2022 / Revised: 30 March 2022 / Accepted: 18 April 2022 / Published online: 24 April 2022

Abstract

In this study, the structure and ionic conductivity behavior of a polymer nanocomposite electrolyte system consisting of poly(ethylene oxide) (PEO), metal–organic framework 5 (MOF-5), and lithium bis(trifluoromethylsulfonyl)imide (LiTFSI) were investigated by using molecular dynamics (MD) simulations. Based on ionic conductivity data from MD simulations, the mobility of Li cations increases in PEO:LiTFSI electrolyte system with the addition of MOF-5. Zn atoms of MOF-5 hold almost three TFSI anions per Zn atom. In addition, when Zn atoms of MOFs and oxygen atoms of PEO interact, four oxygen atoms are saturated per Zn atom. Furthermore, Li cations are stuck among oxygen atoms of PEO as a result of their ionic interactions with O atoms. Positive charges of MOF-5 leads to the separation of Li cations from TFSI anions in PEO:LiTFSI:MOF-5 electrolyte system. In addition, positively charged atoms of MOF-5 interact with oxygen atoms of PEO chains. MOF-5 exhibits acidic surface properties through Zn atoms located close to its surface, and Zn atoms interact with partially negatively charged oxygen atoms of PEO chains and fully negatively charged TFSI anions. Therefore, lithium cations are released. The mobility of Li cations increases due to favorable interactions of MOF-5 with PEO and TFSI anions. The ionic conductivity results verify that nanoparticles like MOF-5 consisting of positively charged atoms can be used to improve the ionic mobility in electrolyte systems which include PEO-like polymers consisting of partially negative charged atoms.

Keywords Poly(ethylene oxide) · Metal–organic framework · MOF-5 · Lithium salt · Polymer electrolyte · Molecular dynamics simulations · Ionic conductivity

Introduction

The rapid developments in smartphone and automotive industries during the twenty-first century increased the importance of energy storage devices. The desire to operate all new devices with electrical energy leads to improvements in their storage units [1–4]. For this reason, battery technologies have a very important role in today's energy storage systems [5–10]. The performance of batteries depends on three important parameters. The first one is high specific energy, the second one is safety, and the third parameter is lifetime. In an ideal battery, each charge and discharge cycle is fully reversible. In practical batteries, the cycle is never completely recyclable and the capacity is lost over time. There are three important parts in batteries. These are cathode, anode, and separator that consist of electrolytes [10–14]. The properties of electrolytes can be improved with the addition of nanoparticles [14, 15]. Electrolytes can be in liquid and solid states [14, 16, 17]. Solid electrolytes are good candidates for property improvement due to their safety, good formability, energy density, and adaptability [14, 18, 19]. The solid electrolytes can be polymer-based electrolytes, inorganic electrolytes, and composite solid electrolytes. There are several types of polymer-based electrolytes such as solid polymer electrolytes, gel/plasticized polymer electrolytes, and composite polymer electrolytes [19–21]. Solid polymer electrolytes are located between anode and cathode structures where they provide ion flow [22, 23]. To

✉ Engin Burgaz
eburgaz@omu.edu.tr

1 Department of Metallurgical and Materials Engineering, Ondokuz Mayis University, Atakum, 55139 Samsun, Turkey

2 Department of Nanoscience and Nanotechnology, Ondokuz Mayis University, Atakum, 55139 Samsun, Turkey

3 Department of Chemistry, Ondokuz Mayis University, Atakum, 55139 Samsun, Turkey

produce efficient solid polymer electrolytes (SPEs), there are critical parameters such as the salt-polymer ratio, degree of crystallinity, thermal stability, mechanical strength, and electrochemical stability [20, 23–25]. Finding the critical salt-polymer ratio to produce SPEs with best efficiency is a very important task to obtain higher ionic conductivity. In addition, nanoparticles can be also incorporated to SPEs to further improve ionic conductivity, thermal stability, mechanical strength, and electrochemical stability [24–29]. Solid polymer electrolytes can be fabricated by using different salt cations due to their different types of applications. Lithium ions are very lightweight cations that could easily flow inside the polymer electrolyte. Therefore, lithium-ion electrolytes are widely used in the literature [30, 31].

SPEs consist of Li or Na salts and typical matrix phases such as poly(ethylene oxide) (PEO) and polypropylene oxide (PPO). However, PPO is not effective as PEO due to its methyl groups that decrease Li mobility in PPO matrix [16, 18]. PEO has oxygen atoms which exhibit partially anionic behavior due to interactions with lithium cations [5, 20, 32–34]. For this reason, lithium cations can easily flow inside the polymer structure [32, 35, 36]. In addition, PEO has a very high dielectric constant and it is a very important property for lithium-ion batteries since high dielectric constant leads to the disassociation of ions in salts [32, 37–39]. Different types of LiX salts (LiTFSI, $LiClO_4$, etc.) can be used in PEO electrolytes to decrease the crystallinity of PEO by increasing segmental motions of PEO chains [17, 25, 34, 39, 40]. LiTFSI is the most commonly used LiX salt because its large TFSI anions can be easily separated from Li cations [4, 10, 39, 41]. Consequently, PEO:LiTFSI complexes are the most widely used electrolytes for Li-ion batteries due to these unique properties of PEO and LiTFSI. However, PEO and lithium salt complexes have very poor ionic conductivity ($\sim 10^{-6}$–10^{-7} S/cm) at room temperature [32, 34, 39]. Metal–organic frameworks (MOFs), silica, and alumina-like nanoparticles can be used to improve the ionic conductivity of PEO and lithium salt complexes [14, 36, 42]. These nanoparticles have Lewis acidic-basic properties that are very important for increasing ionic conductivity [43, 44]. Also, they have large surfaces due to high porosity and those surfaces can enhance the stability of electrolyte/Li interface [45].

MOF structures are cage-like structures in which organic ligands bind inorganic metal ions and ionic clusters together [46–49]. MOFs can be synthesized by using different organic ligands and metal ions [7, 33, 50, 51]. Most MOFs have high surface area, good elasticity, 3D structure, changeable pore size, polarized surface, and ordered microporous structure. These properties are important for gas storage, gas/vapor separation, catalysis, luminescence, drug delivery, and electrochemical applications [50, 52–55]. Among MOFs, metal–organic framework 5 (MOF-5) is the most widely used material due to its excellent porosity and well-ordered cage-like structure, high thermal stability, and tunable chemical functionality [37, 48, 53, 54, 56]. The main reason for its high porosity and thermal stability can be explained such that MOF-5 has a large-firm structure due to its chemical benzene links [52, 57]. MOF-5 which is also known as isoreticular MOF-1 (IRMOF-1) is a cubic structure with ZnO_4 groups that are located on the corners, and these ZnO_4 units are bonded to each other with [O_2C-C_6H_4-CO_2] (1,4-benzenedicarboxylate, BDC) groups [52, 57, 58].

Increasing the lithium mobility among PEO chains is important to develop efficient PEO:LiTFSI electrolytes. Lithium mobility can be increased by separating anions and cations of lithium-containing salt structures. There are several ways to separate the anions and cations of lithium-containing salts such as the addition of nanoparticles, modified ionic liquids (ILs), and ionic salts to the system. Previously, it was found out that pyrrolidinium-based IL functionalized with a short oligoether side chain interacts with PEO chains, detaches lithium cations from PEO chains, and increases the ionic mobility [59]. In another study, the ionic conductivity behavior of a polymer electrolyte system containing PEO and LiTFSI was investigated in detail by using molecular dynamics simulations. According to simulation results, the flow of Li cations slows down near the surface due to accumulation of TFSI anions on the surface [60]. Molinari et al. [61] investigated the behavior of PEO, Li^+, and $TFSI^-$ systems at high salt ratios by using molecular dynamics simulations. Based on the simulation data, they revealed that Li cations and polymer chains interact less frequently in LiTFSI clusters, and Li^+ and $TFSI^-$ ions tend to exhibit asymmetric behavior in which the number of TFSI anions is much larger than that of Li cations. If the amount of anions is high, then the lithium mobility in the system decreases [61]. Brooks et al. [62] created LiTFSI-PEO systems with Li:EO ratios of 0.02, 0.04, 0.06, and 0.08, by using molecular dynamics simulations. According to simulation data, they found out that the most mobile lithium ions exhibit interchain hopping behavior, while the least mobile ones are located between two or more polymer chains [62]. Previously, in a molecular dynamics simulation study, 1-ethyl-3-methylimidazolium (EMIm)-TFSI ionic liquid was added to the PEO/LiTFSI system (Li:EO, 1:16) and the flow of Li cations in the system was examined in detail. Based on the results, it was reported that Li cations move away from TFSI anions and interact with PEO chains; thus, the movement of PEO chains increases with the addition of IL [63]. Previously, in an experimental study, electrolyte samples consisting of LiTFSI, 1-butyl-3-methylimidazolium bis(trifluoromethanesulfonyl)imide (BMIMTFSI) IL, and PEO were prepared. According to experimental data, it was revealed that PEO electrolytes consisting of LiTFSI and BMIMTFSI display higher ionic conductivity compared to

PEO/LiTFSI electrolytes due to ionic interactions between 1-butyl-3-methylimidazolium bromide (BMIM) cations and TFSI anions [64]. Earlier on, Shin et al. [41] studied the ionic conductivity behavior of PEO/LiTFSI polymer electrolyte consisting of 1-methylpyrrolidine with 1-iodopropane TFSI ($PYR_{13}TFSI$). PEO/LiTFSI structure without IL exhibited lower ionic conductivity than that of PEO/LiTFSI/$PYR_{13}TFSI$ due to less ionic mobility of Li cations. The reason behind these results was explained such that Li cations were trapped between oxygen atoms of EO. With IL addition, the ionic mobility of Li cations increases and lithium cations are separated from TFSI anions because of interactions between PYR cations and TFSI anions inside the polymer electrolyte [41].

MOFs are widely used in polymer electrolytes since MOF structures increase amorphous content and the ionic conductivity of system [43, 54, 65]. Also, MOF structures can increase the thermal stability of polymer electrolytes because the interactions between MOFs and polymer chains might slow down the polymer mobility. Thus, this behavior could create an effective thermal blockade within the system due to rigid and thermally stable structure of MOFs [54, 66–71]. According to an experimental study, the addition of 5 wt% Al-MOF nanorods to LiTFSI:PEO electrolyte increases the ionic conductivity because the crystallinity decreases and Lewis acidic groups on MOFs could increase the degree of Li^+ separation from large TFSI anions [71]. Previously, it was shown that the addition of 10 wt% magnesium-benzene tricarboxylate MOF (Mg-BTC MOF) to PEO:LiTFSI increases the ionic conductivity by 2 orders of magnitude at 20 °C. The main reason behind this result can be explained such that Lewis acid–base interactions diminish ionic coupling and increase salt disassociation and thus the mobility of Li cations [66]. Dutta and Kumar [72] prepared PEO electrolytes consisting of Cu-based MOFs and BMIM and revealed that the crystallinity decreases due to the complexation of $BMIM^+$ with oxygen atoms with an increasing amount of BMIM [72]. Formerly, it was found out that the addition of copper benzene dicarboxylate-MOF (Cu BDC-MOF) to PEO:LiTFSI increases the ionic conductivity and thermal stability. The reason for higher ionic conductivity was discussed such that positively charged Cu atoms of MOF interact with negatively charged PEO oxygen atoms and TFSI anions [70]. In another study, it was shown that the addition of Zr-based MOF UIO-66 whose backbone was modified with amine and 1,4-benzene dicarboxylic acid (BDC) to PEO:LiTFSI improved the ionic conductivity due to the strong electronic donating group of amine (NH_2) compared to pure PEO electrolyte [73]. Previously, Angulakshmi et al. studied PEO:LiTFSI electrolytes consisting of UiO-66-NH_2@SiO_2 MOF nanostructures and found out that the ionic conductivity at 70 °C increases by 2 orders of magnitude with the addition of 10 wt% UiO-66-NH_2@SiO_2 compared to that of pure PEO:LiTFSI. The reason behind this improvement was explained such that the microporous structure of UiO-66-NH_2@SiO_2 MOF creates suitable ion conduction channels and thus enhances Li mobility throughout PEO matrix [55]. Formerly, in an experimental study, it was revealed that PEO:LiTFSI electrolytes consisting of 10 wt% MOF-derived Co-doped carbon nanocage structure and LiTFSI/EMIM-TFSI increased the ionic conductivity at room temperature compared to non-modified MOF containing electrolyte [49]. Among all MOF structures, MOF-5 is the most widely used Zn-based MOF due to its extra-high porosity and ordered structure, high thermal stability, and flexible chemical functionality [37, 52, 56, 74]. Previously, Yuan et al. [56] revealed that PEO-$LiN(SO_2CF_3)_2$ electrolytes (EO:Li = 10:1) containing 10 wt% MOF-5 display 3.16×10^{-5} S/cm at 25 °C. The main reason behind this enhancement was explained such that Li-ion conduction channels are formed in PEO matrix which speed up the ion transportation compared to pure PEO electrolyte. In addition, it was also shown that EO:Li = 10:1 is the critical ratio to increase ion mobility in PEO electrolytes containing 10 wt% MOF-5 [56].

As mentioned earlier, when polarizing additives such as ionic liquids and partially positive charge containing MOF-5-like nanoparticles are added to PEO:LiTFSI structures, the ionic mobility in the system increases due to the freeing of Li cations from TFSI and PEO chains. PEO-like polymers that contain partially negative charge atoms could hold some lithium cations. The ion mobility decreases in PEO:LiTFSI electrolyte if LiTFSI salt amount is not enough to saturate oxygen atoms of PEO chains [59–62]. To increase the ion mobility in PEO:LiTFSI electrolytes, nanoparticles that include partially positive charge atoms could lead to the separation of Li cations from PEO chains and TFSI anions. In this study, a nanocomposite electrolyte system consisting of PEO, LiTFSI, and MOF-5 was studied by using molecular dynamics simulations. In this work, specifically, the molecular interactions between (i) Li cations and oxygen atoms of PEO, (ii) Li cations and TFSI anions, (iii) zinc atoms of MOF-5 and oxygen atoms of PEO, and (iv) zinc atoms of MOF-5 and nitrogen atoms of TFSI were investigated. The effects of these interactions on ionic conductivity were studied to reveal how Lewis acidic surfaces (partially positive charge atoms on the surface) of MOF-5 increase the ionic conductivity by separating Li cations from TFSI anions and freeing Li cations from locations between PEO chains. The specific purpose of this work is to find out how the LiTFSI weight ratio (Li cation amount and TFSI anion amount) affects the ion mobility in the system by saturating oxygen atoms of PEO and zinc atoms of MOF-5.

Theoretical calculations

PEO, LiTFSI, and MOF-5 structures were created by means of the Accelrys commercial software (Materials Studio 7.0). Polymer electrolyte systems were built by means of the amorphous builder module. The systems consisted 23 PEO chains, which have 100 EO monomers per PEO chain, 66 and 88 LiTFSI molecules (could change by weight percentage), and 1 MOF-5 molecule (Table 1) (Fig. S1). Then, the system energy levels were reduced by geometry optimization under COMPASS II force field [75, 76].

The systems were pressured under 0.5 GPa and heated to 298 K for 5 ps to remove the gaps in the systems. Dynamics module used to collect Li cation mobility data from the systems under 298 K, 308 K, 328 K, and 338 K temperature (Nose thermostat) and 0.1 GPa (Berendsen barostat) for 10,000 ps. After dynamics results, mean-square displacement ($Å^2$)–time (ps) graphs were obtained to calculate diffusion coefficient and ionic conductivity. After obtaining MSD values, ionic conductivity values were calculated from diffusion coefficient values by using the Nernst-Einstein equation. Slope values were obtained from MSD graphs. The diffusivity (D) formula is expressed as in the following:

$$D = \frac{1}{6N}\lim_{t\to\infty}\frac{d}{dt}\sum_{i=1}^{N}\left\langle\left[r_i(t) - r_i(0)\right]^2\right\rangle \tag{1}$$

The parts inside the limit term are equal to the MSD slope multiplied by N. Thus, Eq. (1) is converted to Eq. (2) as in the following:

$$D = \frac{1}{6N}MSD.N \tag{2}$$

Then, the diffusivity equation is converted to Eq. (3)

$$D = \frac{MSD}{6} \tag{3}$$

Then, the diffusion coefficient values are converted to ionic conductivity values by using the Nernst-Einstein equation at Eq. (4) [77–80].

$$\sigma = \frac{Nz^2e^2D}{VkT} \tag{4}$$

Table 1 Types and number of particles in the system

Sample name	Li-TFSI	PEO (100 monomers)	MOF-5
15Li	66	23	
20Li	88	23	
15Li-5MOF	66	23	1
20Li-5MOF	88	23	1

where σ is the ionic conductivity, e is the electron charge (1.6×10^{-19} C), V is the volume of simulation cell ($Å^3$), k is Boltzmann's constant (1.38×10^{-23} $m^2/kg/s^2/K$), T is the temperature (K), and z represents the total charge within the units [81].

Radial distribution functions were used to calculate the coordination number of atoms for Li–O, Li-TFSI, Zn–O, Zn-TFSI, Zn-F, and Zn-N interactions and distributions for every unit in the system. Value for $g(r)$ can be used to calculate the coordination number with Eq. (5)

$$n_{A\ldots B}(\Gamma) = 4\pi\frac{N_B}{(V)}\int_0^{\Gamma} g_{A\ldots B}(\Gamma)\Gamma^2 dr \tag{5}$$

where $n_{A\cdots B}(r)$ is the number of A particles coordinated with B particles within a radius (r), V is the volume of the cell, N_B is the total number of B particles in the system, and $g_{A\cdots B}(r)$ is the pair correlation function between A and B [77, 82–84].

Results and discussion

Structural characterization

To determine the structural effects of MOF on the PEO:LiTFSI system, the radial distribution function (RDF) that was calculated between Li and O atoms for all samples is shown in Fig. 1. The peak value of minimum interaction distance (r_{min}) between Li and O atoms was found to be 1.93 Å for the 20Li-5MOF system based on the RDF graph. However, on the other hand, r_{min} values between Li and O atoms for 15Li, 20Li, and 15Li-5MOF were found to be 1.47 Å. These results showed that the r_{min} value between Li and O atoms for 20Li-5MOF is much bigger compared to that of other three PEO:LiTFSI systems. The increase of atomic distance promotes a decrease of atomic interaction between Li and O atoms, so the mobility of Li cations increases in the 20Li-5MOF system. In 15Li, 20Li, and 15Li-5MOF systems, smaller r values between Li and O atoms lead to higher coordination complex numbers ($g(r)$ value is about 9). This result shows that O atoms inside 15Li, 20Li, and 15Li-5MOF systems hold more Li ions and leads to much less Li mobility.

The coordination numbers for Li–O interaction in all samples are shown in Table 2. Coordination numbers of 15Li, 20Li, 15Li-5MOF, and 20Li-5MOF were calculated to be 1.79, 1.77, 1.84, and 0.56, respectively. Based on this data, the coordination number between Li and O atoms inside the system decreases when Li and MOF percentages increase in the system. The MOF structure has Zn atoms that could hold TFSI anions and create an opportunity to move Li cations freely in 15Li-5MOF and 20Li-5MOF. It was previously

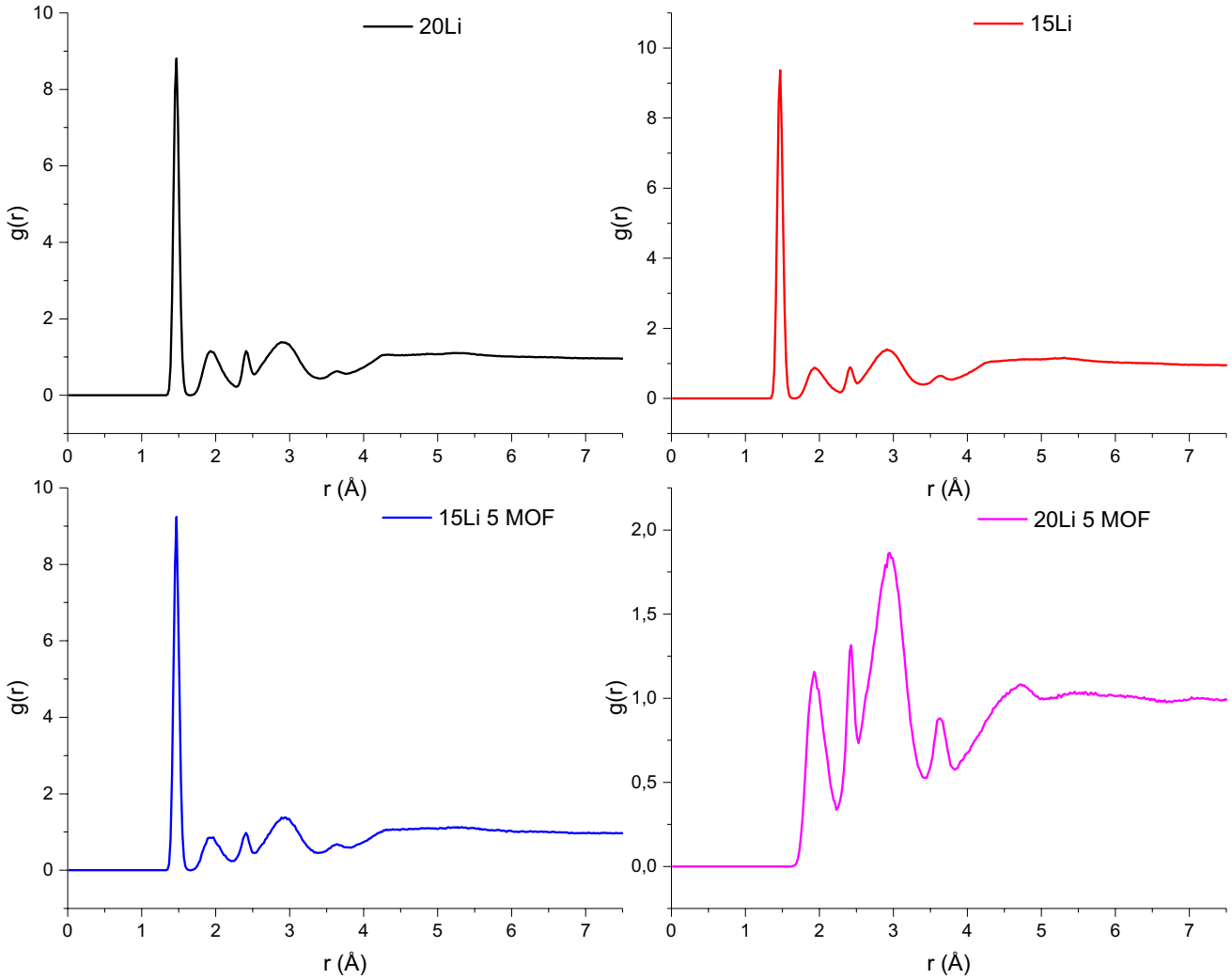

Fig. 1 RDF analysis of all Li–O interactions between Li cations and O atoms of TFSI anions, PEO chains, and MOF-5

Table 2 Li–O interactions between Li cations and all oxygen atoms inside the system

Sample name	$g(r)$	r_{min} (Å)	V (Å^3)	Number of O particles	Coordination number
15Li	8.80	1.47	159,277.002	2432	1.79
20Li	8.81	1.47	164,287.052	2476	1.77
15Li-5MOF	9.24	1.47	166,329.238	2484	1.84
20Li-5MOF	1.15	1.93	155,541.595	2528	0.56

shown that Zn^{2+} cations of MOF interact with both TFSI anions and O atoms of PEO chains. This outcome reduces the crystallization of PEO and improves the ionic conductivity of system [56, 66, 85]. Also, Li mobility enhances through complexation of Li cations with oxygen atoms of PEO chains [39]. However, on the other hand, the ionic conductivity decreases when the amount of PEO increases in the PEO electrolyte system. The oxygen atoms of PEO chains can establish more oxygen-lithium complexes due to a high percentage of PEO [62]. In 15Li-5MOF, non-conductive PEO oxygen atoms can hold more Li cations and decrease ion mobility due to 80% PEO amount. As a result, 15Li-5MOF has less ion movement compared to 20Li-5MOF. However, in contrast, high amount of Li and low percentage of PEO in 20Li-5MOF lead to the formation of less coordination number compared to 15Li-5MOF.

Figure 2 shows the RDF graph between Li cations and O atoms of PEO chains. r_{min} values between Li and O atoms of PEO for 15Li, 20Li, and 15Li-5MOF were found to be 1.47 Å. However, on the other hand, the r_{min} value between Li and O atoms of PEO for 20Li-5MOF is 1.93 Å. Based on these results, the minimum interaction distance between Li and O atoms of PEO in 20Li-5MOF is much larger compared to other sample compositions. Thus, the Li mobility in 20Li-5MOF is much higher than 15Li, 20Li

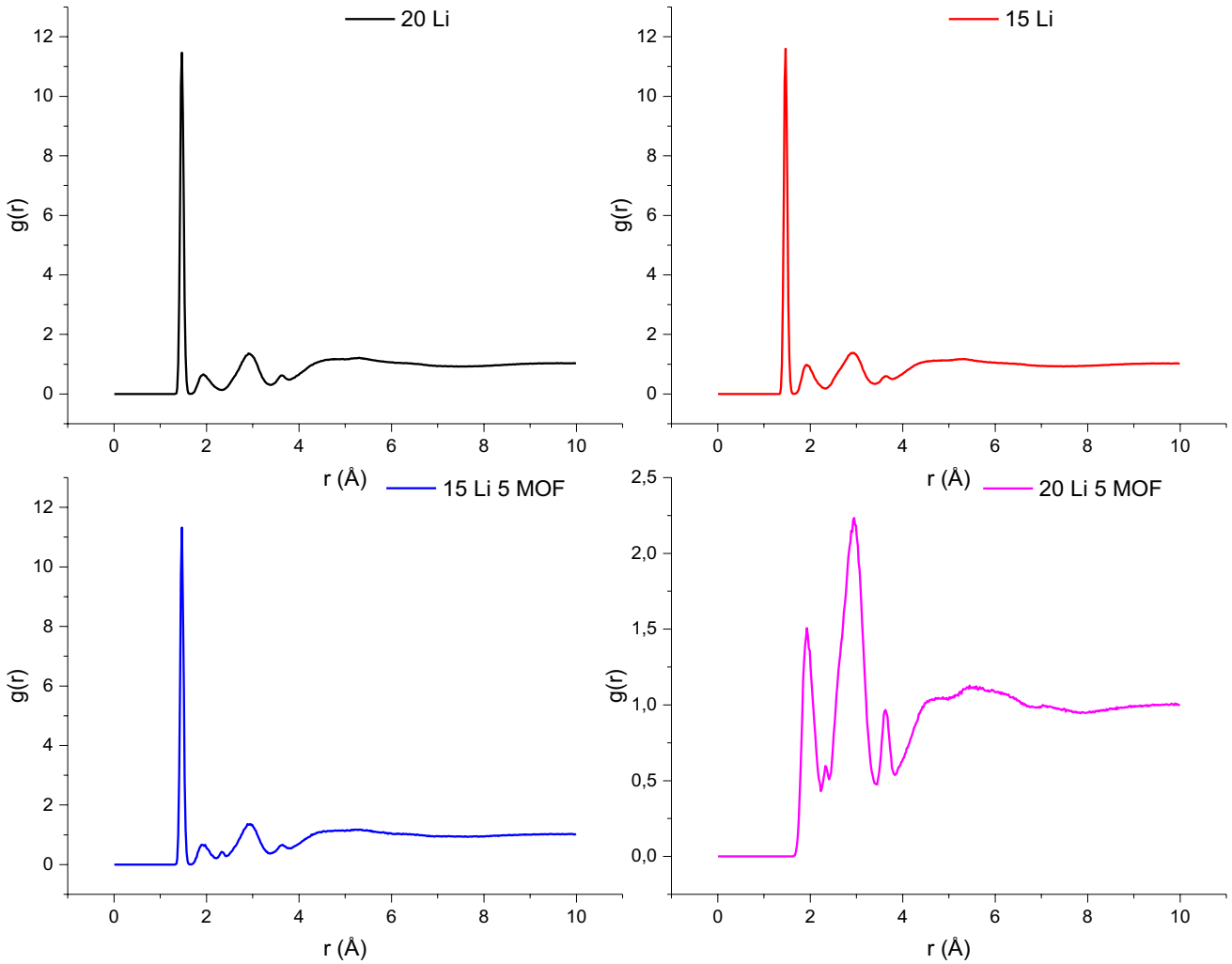

Fig. 2 RDF analysis of Li–O interactions between Li cations and O atoms of PEO chains

and 15Li-5MOF. The coordination number in 20Li-5MOF decreases since the amount of Li cations per oxygen in PEO chains increases much more compared to 15Li, 20Li, and 15Li-5MOF. Also, Fig. S3 and Fig. S4 show the configurations for interactions between one and two Li cations and O atoms of three EO repeating units on PEO chains before dynamic and after dynamic tests.

In Table 3, coordination numbers that belong to Li cations and O atoms of PEO chains in 15Li, 20Li, 15Li-5MOF, and 20Li-5MOF were calculated to be 2.20, 2.16, 2.27, and 0.73, respectively. Based on this data, the coordination number between O atoms of PEO chains and Li cations decreases when the amount of Li increases in samples that do not contain MOF. Moreover, the coordination number drastically decreases when the amount of Li increases in samples consisting of MOF. The reason behind this decrease can be explained such that interactions between Zn atoms of MOF and O atoms of PEO chains in samples containing MOF reduce the number of interactions between Li cations and O atoms of PEO chains. Thus, this outcome leads to the escape of Li cations from coordination sites between Li and O atoms of PEO and reduction in the probability of coordination between Li and O atoms of PEO. All steps in this

Table 3 Li–O interactions between Li cations and O atoms of PEO chains inside the system

Sample name	$g(r)$	r_{min} (Å)	V (Å^3)	Number of O particles	Coordination number
15Li	11.47	1.47	159,277.002	2300	2.20
20Li	11.6	1.47	164,287.052	2300	2.16
15Li-5MOF	12.34	1.47	166,329.238	2300	2.27
20Li-5MOF	1.65	1.93	155,541.595	2300	0.73

mechanism help to move Li cations throughout PEO chains and increase Li mobility in the system.

Figure 3 shows the interaction of three ethylene oxide monomers with one Li cation and two Li cations. In Fig. 3a, one Li cation is surrounded by three oxygen atoms and the total charge of this possible configuration is − 0.5e. Because of this negative total charge, three oxygen atoms drag the Li cation toward themselves and this configuration is stable. In Fig. 3b, two Li cations are surrounded by three oxygen atoms and the total charge of this possible configuration is + 0.5e. Because of this positive total charge, three oxygen atoms could not drag Li cations toward themselves. As a result, two Li cations are separated from this unstable configuration.

Figure 4 shows RDF graphics of Li-TFSI interactions especially between Li cations and N atoms inside the system. Minimum interaction distances of Li-TFSI in 15Li, 20Li, 15Li-5MOF, and 20Li-5MOF were found to be 1.35 Å for all samples. The $g(r)$ value of at r_{min} 15Li and 15Li-MOF is the highest since their coordination numbers are the highest among sample compositions. Increasing the amount of LiTFSI in samples without MOF decreases the $g(r)$ value at the minimum interaction distance. The $g(r)$ values at r_{min} in both 20Li-5MOF and 20Li samples are very close to each other. The lowest $g(r)$ value of at r_{min} between Li and TFSI was found for 20Li-5MOF. The addition of MOF to the PEO:LiTFSI electrolyte system increases the amount of cavity due to the porous structure of MOF [51, 56, 66, 85]. Also, O and Zn atoms of MOF could interact with Li cations and TFSI anions, respectively. Consequently, the $g(r)$ value at the minimum interaction distance between Li and TFSI decreases when MOF is added to the electrolyte system. Here, − 1e charged TFSI anions are attracted by + 2e charged Zn atoms of MOF. Therefore, the probability of having TFSI around Li decreases. In addition, − 0.5e charged O atoms of MOF can also interact with + 1e charged Li cations [51, 56, 66, 85]. In Table 4, O and Zn atoms of MOF structure have − 0.5e average charge and + 2e charge, respectively. Hence, the interaction between O atoms and Li cations is not strong enough to hold Li. However, the charge that belongs to Zn atoms is strong enough to retain − 1e charged TFSI structure. Based on these results, it is confirmed that the presence of MOF structure in the PEO:LiTFSI electrolyte system could help to the separation of Li cations and TFSI anions [51, 56, 66, 85].

In Table 5, coordination numbers that belong to Li cations and TFSI anions in 15Li, 20Li, 15Li-5MOF, and 20Li-5MOF were calculated to be 0.32, 0.30, 0.31, and 0.29, respectively. Based on this data, interactions between Li cations and TFSI anions decrease with the addition of MOF to the system. Although the decrease in coordination numbers is not much high, the addition of MOF to the system facilitates the separation of Li cations from TFSI anions. The main reason behind this observation can be explained such that Zn atoms of MOF attract TFSI anions toward themselves [51, 56, 66, 85].

The coordination numbers for the Zn–O interaction in samples containing MOF are shown in Table 6. Coordination numbers of 15Li-5MOF and 20Li-5MOF were calculated to be 1.88 and 3.56, respectively. Based on this data, the coordination number between Zn and O atoms inside the system increases when Li percentage increases in the system. There is a high coordination number between oxygen atoms of PEO and zinc atoms of MOF structure in MOF-containing PEO electrolyte samples compared to the system without MOF (Supporting information Fig. S5). Due to this high Zn–O interaction, charge effects of oxygen atoms on Li cations are weakened. This outcome allows Li cations to move more easily within the structure. In Table 7, it is seen that Zn atoms of MOF and O atoms of PEO in 20Li-5MOF have a much higher coordination number compared to 15Li-5MOF. This high coordination number value leads to the decrease of charge on oxygen atoms and can provide better cation mobility in 20Li-5MOF.

The coordination numbers for Zn and oxygen atoms of PEO in samples containing MOF are shown in Table 7. Coordination numbers of 15Li-5MOF and 20Li-5MOF were calculated to be 2.34 and 4.13, respectively. The interaction between O atoms of PEO and Zn atoms in 20Li-5MOF is much higher compared to that of 15Li-5MOF. This ensures that the negative charge on oxygen atoms of PEO

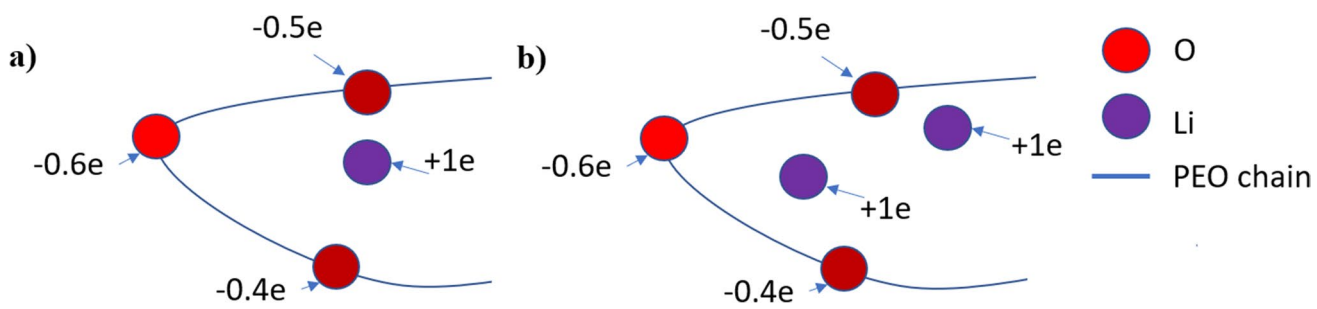

Fig. 3 The interaction of three ethylene oxide monomers with **a** one Li cation and **b** two Li cations (Supporting information Figs. S2 and S3)

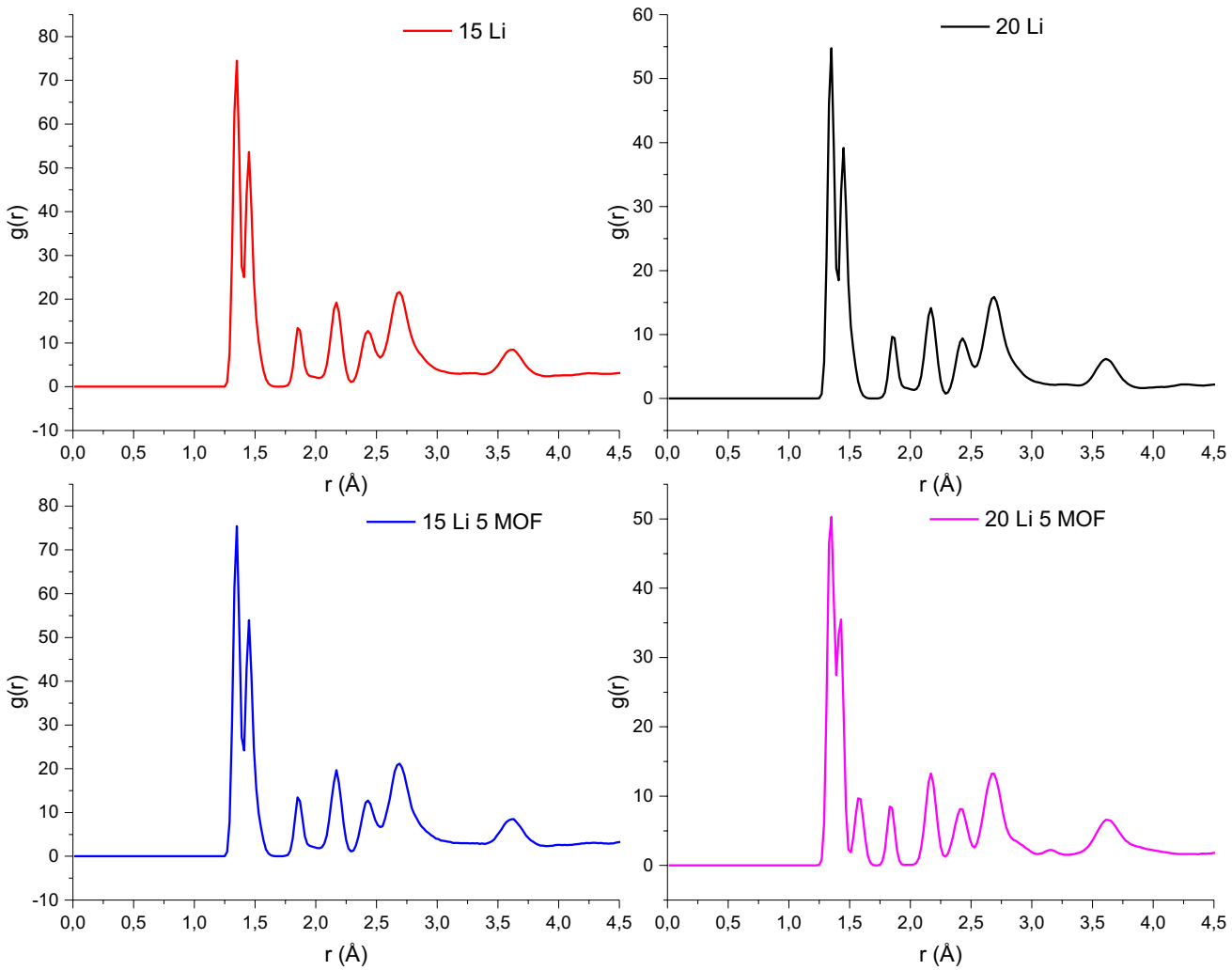

Fig. 4 RDF analysis of Li-TFSI interactions in the system

Table 4 Charge values of Zn, O, Li, and TFSI as a result of the interaction of MOF-LiTFSI

Charged atoms and molecules	Zn	O	Li	TFSI
Electronic charges	+2	−0.4 to −0.6	+1	−1

Table 5 Li-TFSI interactions between Li cations and TFSI anions

Sample name	$g(r)$	r_{min} (Å)	V (Å^3)	Number of TFSI particles	Coordination number
15Li	74.5	1.35	159,277.002	66	0.32
20Li	54.8	1.35	164,287.052	88	0.30
15Li-5MOF	75.4	1.35	166,329.238	66	0.31
20Li-5MOF	50.35	1.35	155,541.595	88	0.29

Table 6 Zn–O interactions between Zn atoms of MOF and all oxygen atoms inside the system

Sample name	$g(r)$	r_{min} (Å)	V (Å^3)	Number of O particles	Coordination number
15Li-5MOF	9.47	1.47	166,329.23	2484	1.88
20Li-5MOF	2.04	2.95	155,541.59	2528	3.56

Table 7 Zn–O interactions between Zn atoms of MOF and O atoms of PEO inside the system

Sample name	$g(r)$	r_{min} (Å)	V (Å^3)	Number of O particles	Coordination number
15Li-5MOF	12.7	1.47	166,329.238	2300	2.34
20Li-5MOF	2.65	2.93	155,541.595	2300	4.13

is weakened by Zn atoms. Therefore, this result allows Li cations in 20Li-5MOF to have better ion mobility compared to 15Li-5MOF. On the other hand, in 15Li-5MOF, Zn atoms of MOF again establish a coordinated interaction with O atoms of PEO. Although this interaction is not as strong as that of 20Li-5MOF, it still positively affects Li mobility in 15Li-5MOF.

The coordination numbers for the Zn-N interaction in samples containing MOF are shown in Table 8. Coordination numbers of 15Li-5MOF and 20Li-5MOF were calculated to be 2.81 and 2.41, respectively. Based on this data, the coordination number between Zn and N atoms inside the system decreases when Li and N percentages increase in the system. Coordination numbers between Zn and N atoms are very close for both systems. However, the coordination number in 15Li-5MOF is slightly higher compared to that in 20Li-5MOF. The decrease of coordination number in 20Li-5MOF is caused by a higher number of N atoms. This means that establishing an interaction is more difficult for Zn atoms to coordinate with nitrogen due to the presence of a higher number of N atoms in 20Li-5MOF. Another reason behind this outcome can be explained such that positive charges of Zn atoms are not strong enough to coordinate with the higher number of N atoms. The small difference in coordination numbers between these two sample compositions shows that Zn and N atoms in both samples interact in a very similar manner. In both sample compositions, the stronger interaction between Zn and N atoms leads to the weakening of interaction between N atoms and Li cations. Figure 5 shows the interaction between Zn atoms of MOF and TFSI anions in 15Li-5MOF and 20Li-5MOF. Here, + 2e positive charges on Zn atoms interact with − 1e negative charges of TFSI anions. In Fig. 5, the decrease of ionic interaction between Li cations and TFSI anions is specifically shown. The weakening of this interaction is basically facilitated by the fact that TFSI anions are attracted by Zn atoms of MOF structure. For this reason, the mobility of Li cations increases in sample compositions such as 15Li-5MOF and 20Li-5MOF.

In Table 9, coordination numbers of Zn atoms of MOF and F atoms of TFSI anions were calculated to be 11.83 and 12.07 at a distance of 2.17 Å for 15Li-5MOF and 20Li-5MOF, respectively. Looking at coordination numbers in Zn-F interaction, there are six F atoms associated with each TFSI anion. In other words, there is a good amount of interaction between Zn atoms of MOF and two TFSI anions in 15Li-5MOF and 20Li-5MOF at a distance of 2.17 Å. Although there is not much difference in the coordination number between 15Li-5MOF and 20Li-5MOF, Zn-F

Table 8 Zn-N interactions between Zn atoms of MOF and N atoms of TFSI anions inside the system

Sample name	$g(r)$	r_{min} (Å)	V (Å^3)	Number of N particles	Coordination number
15Li-5MOF	47.45	3.29	166,329.238	66	2.81
20Li-5MOF	28.61	3.29	155,541.595	88	2.41

Table 9 Zn-F interactions between Zn atoms of MOF and F atoms of TFSI anions inside the system

Sample name	$g(r)$	r_{min} (Å)	V (Å^3)	Number of F particles	Coordination number
15Li-5MOF	116.1	2.17	166,329.238	396	11.83
20Li-5MOF	83.1	2.17	155,541.595	528	12.07

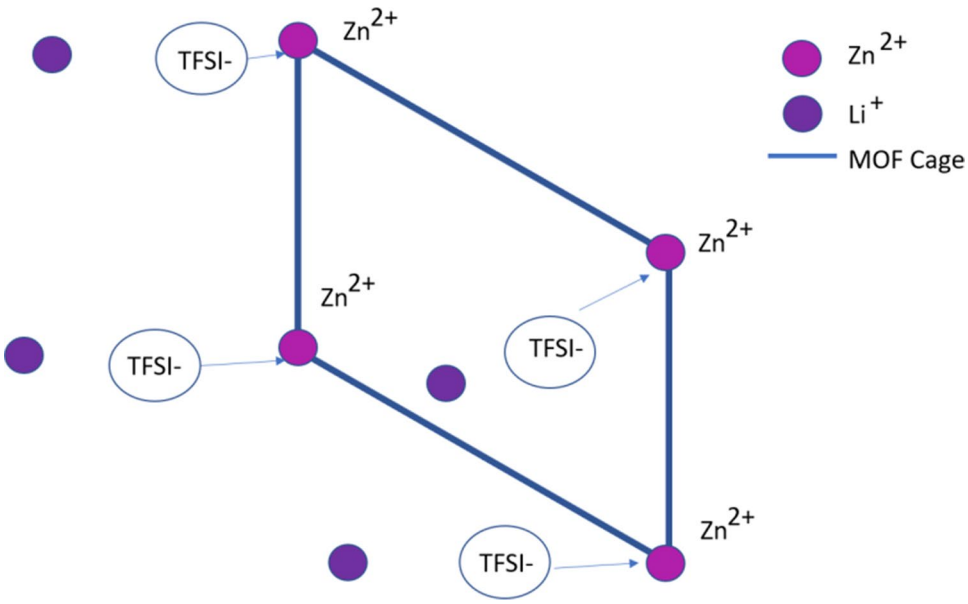

Fig. 5 The interaction between Zn atoms of MOF and TFSI anions in 15Li-5MOF and 20Li-5MOF (Supporting information Fig. S6, Fig. S7, and Fig. S8)

interaction in 20Li-5MOF is slightly higher than that in 15Li-5MOF. This outcome does not affect the mobility of Li cations in 20Li-5MOF very much since there is no difference in the number of coordinating atoms between two sample compositions.

Diffusion coefficient calculations

The diffusion coefficient values of 15Li, 20Li, 15Li-5MOF, and 20Li-5MOF were calculated at a temperature range of 298–338 K via molecular dynamics simulations. The results are shown in Fig. 6. The highest diffusion coefficient values in 15Li, 20Li, 15Li-5MOF, and 20Li-5MOF were calculated to be 2.57×10^{-12} m^2/s, 2.27×10^{-12} m^2/s, 2.95×10^{-12} m^2/s, and 3.31×10^{-12} m^2/s at 338 K, respectively. Based on these results, diffusion coefficients increase when Li concentration increases in 15Li-5MOF and 20Li-5MOF. The number of TFSI anions increases with the increase of Li cations in the system. The mobility of Li cations decreases due to interactions between Li and TFSI. This is the reason behind the fact that diffusion coefficients do not increase in parallel with the increase of Li concentration in 15Li and 20Li systems. The diffusion coefficients of PEO electrolyte samples increase with an increasing concentration of MOF. The main reason for the increase of diffusion coefficients is the acidic behavior of Zn atoms in MOF which separates Li cations and TFSI anions. In addition, cavities are formed in the system due to the porous structure of MOF.

Ionic conductivity calculations

Ionic conductivity values of 15Li, 20Li, 15Li-5MOF, and 20Li-5MOF were calculated at a temperature range of 298–338 K via molecular dynamics simulations. The results for ionic conductivity calculation are shown in Fig. 7. Based on these results, ionic conductivity increases when Li concentration increases in the system. The ionic conductivity values of 15Li and 20Li at 338 K were found to be 2.49×10^{-5} S/cm and 3.32×10^{-5} S/cm, respectively. When these simulation results are compared with experimental data in the literature, conductivity values of 15Li and 20Li simulation cells are about ten times lower at all temperature values [54]. However, it is known that the density value of system is approximately 1.24 g/cm^3 in the experimental data [54, 61–64]. For this reason, simulation tests of the system were carried out under 0.1 GPa pressure to ensure this density value. This high-pressure value can affect the ion mobility [86]. In addition, the number of Li cations in the simulation system is much less than that of experimental systems [62]. Since the size of experimental systems is much larger than that of simulation systems, sample regions in which Li cations have ion mobility are greater [56, 62]. Due to the size of system and the large number of Li cations in experiments, there may be differences between simulation values and experimental data. However, the compatibility of simulation data within itself makes the simulation results acceptable.

Adding MOF-5 to PEO:LiTFSI electrolytes increases the distance between PEO chains and creates a porous structure in the system (Fig. S5) [51, 56, 66, 85]. This outcome allows Li cations to move faster in the system. Moreover, zinc atoms of MOF and oxygen atoms of PEO interact with each other due to the + 2e charge of zinc atoms and the negative charge behavior of oxygen atoms [51, 56, 66, 85]. As a result of this interaction, PEO chains move toward the MOF structure. The charges on oxygen

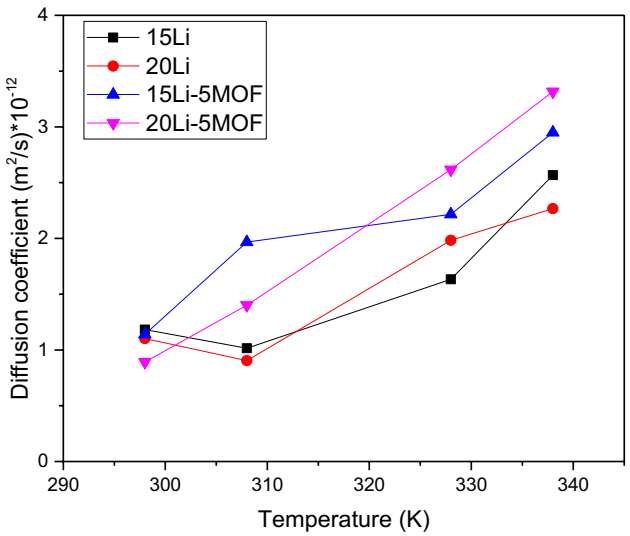

Fig. 6 Diffusion coefficient calculations of all system cells

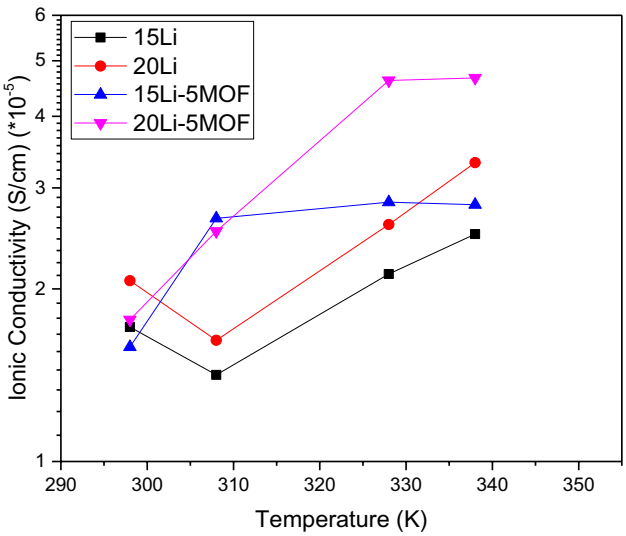

Fig. 7 Ionic conductivity calculations of all system cells

atoms of PEO chains weaken, and the tendency of oxygen atoms to hold Li cations decreases due to their interactions with zinc atoms of MOF. The decrease in their tendency to hold Li cations also enables Li cations to move freely in the system [51, 56, 66, 85]. In the structural analysis of Table 3, there is more coordination number between Zn and O atoms in 20Li-5MOF compared to 15Li-5MOF. This outcome directly affects the ionic movement since Zn atoms can hold more O atoms in 20Li-5MOF. PEO:LiTFSI electrolytes consisting of 5% MOF display better ionic conductivity compared to PEO:LiTFSI electrolytes without MOF. Thus, the presence of MOF inside the PEO:LiTFSI electrolyte system leads to the improvement of ionic mobility. For this reason, structural analysis results of MD simulations (Zn–O and Zn-LiTFSI interactions) and ionic conductivity results of MD simulations have reasonable relationships between them.

Conclusions

In this work, the structural analysis and ionic conductivity behavior of the PEO:LiTFSI system consisting of MOF-5 nanoparticles were investigated by using molecular dynamics simulations. The ionic conductivity of PEO-based polymer electrolytes could be improved with the addition of MOF-5 nanoparticles with Lewis acidic surface. Based on simulation results, it was found out that some Li cations are retained by oxygen atoms of PEO as a result of ionic interactions between oxygen atoms of PEO and Li cations. The addition of MOF-5 nanoparticles with Zn positive charges to the PEO:LiTFSI electrolyte system helps the separation of Li cations from TFSI anions. Based on ionic conductivity data from MD simulations, the mobility of Li cations increases in the PEO:LiTFSI electrolyte system with the addition of MOF-5. Considering interactions of MOF-5 structure with PEO chains and TFSI anions, Zn atoms of MOF-5 interact with partially negatively charged oxygen atoms of PEO chains and fully negatively charged TFSI anions. As a result of these interactions, Zn atoms of MOF-5 hold almost three TFSI anions per Zn atom. In addition, when Zn atoms of MOFs and oxygen atoms of PEO interact, four oxygen atoms are saturated per Zn atom. This behavior increases the movement of Li cations in the electrolyte system. Based on ionic conductivity results, the ionic conductivity values of PEO:LiTFSI electrolytes without MOF-5 are much lower compared to those consisting of MOF-5. In conclusion, these results verify that nanoparticles like MOF-5 consisting of positively charged atoms and Lewis acidic surface behavior can be used to improve the ionic conductivity of electrolyte systems which contain PEO-like polymers consisting of partially negative charged atoms and LiTFSI-like salts.

Supplementary Information The online version contains supplementary material available at https://doi.org/10.1007/s11581-022-04580-w.

Acknowledgements The use of facilities in the Department of Metallurgical and Materials Engineering at Ondokuz Mayis University is acknowledged.

References

1. Xiang Y, Li J, Lei J, Liu D, Xie Z, Qu D, Li K, Deng T, Tang H (2016) Advanced separators for lithium-ion and lithium–sulfur batteries: a review of recent progress. Chemsuschem 9:3023–3039. https://doi.org/10.1002/cssc.201600943
2. Barghamadi M, Kapoor A, Wen C (2013) A review on Li-S batteries as a high efficiency rechargeable lithium battery. J Electrochem Soc 160:A1256–A1263. https://doi.org/10.1149/2.096308jes
3. Park M, Zhang X, Chung M, Less GB, Sastry AM (2010) A review of conduction phenomena in Li-ion batteries. J Power Sources 195:7904–7929. https://doi.org/10.1016/j.jpowsour.2010.06.060
4. Zhang H, Li C, Piszcz M, Coya E, Rojo T, Rodriguez-Martinez LM, Armand M, Zhou Z (2017) Single lithium-ion conducting solid polymer electrolytes: advances and perspectives. Chem Soc Rev 46:797–815. https://doi.org/10.1039/c6cs00491a
5. Arya A, Sharma AL (2017) Insights into the use of polyethylene oxide in energy storage/conversion devices: a critical review. J Phys D Appl Phys 50:443002. https://doi.org/10.1088/1361-6463/aa8675
6. Zhao CZ, Duan H, Huang JQ, Zhang J, Zhang Q, Guo YG, Wan LJ (2019) Designing solid-state interfaces on lithium-metal anodes: a review. Sci China Chem 62:1286–1299. https://doi.org/10.1007/s11426-019-9519-9
7. Ye F, Liao K, Ran R, Shao Z (2020) Recent advances in filler engineering of polymer electrolytes for solid-state Li-ion batteries: a review. Energy Fuels 34:9189–9207. https://doi.org/10.1021/acs.energyfuels.0c02111
8. Manthiram A (2017) An outlook on lithium ion battery technology. ACS Cent Sci 3:1063–1069. https://doi.org/10.1021/acscentsci.7b00288
9. Erickson EM, Ghanty C, Aurbach D (2014) New horizons for conventional lithium ion battery technology. J Phys Chem Lett 5:3313–3324. https://doi.org/10.1021/jz501387m
10. Appetecchi GB, Croce F, Persi L, Ronci F, Scrosati B (2000) Transport and interfacial properties of composite polymer electrolytes. Electrochim Acta 45:1481–1490. https://doi.org/10.1016/S0013-4686(99)00363-1
11. Zubi G, Dufo-López R, Carvalho M, Pasaoglu G (2018) The lithium-ion battery: state of the art and future perspectives. Renew Sustain Energy Rev 89:292–308. https://doi.org/10.1016/j.rser.2018.03.002
12. Zhou G, Li F, Cheng HM (2014) Progress in flexible lithium batteries and future prospects. Energy Environ Sci 7:1307–1338. https://doi.org/10.1039/c3ee43182g
13. Fergus JW (2010) Ceramic and polymeric solid electrolytes for lithium-ion batteries. J Power Sources 195:4554–4569. https://doi.org/10.1016/j.jpowsour.2010.01.076
14. Croce F, Appetecchi GB, Persi L, Scrosati B (1998) Nanocomposite polymer electrolytes for lithium batteries. Nature 394:456–458. https://doi.org/10.1038/28818
15. Yao P, Yu H, Ding Z, Liu Y, Lu J, Lavorgna M, Wu J, Liu X (2019) Review on polymer-based composite electrolytes for lithium batteries. Front Chem 7:1–17. https://doi.org/10.3389/fchem.2019.00522

16. Bekaert E, Buannic L, Lassi U, Llordés A, Salminen J (2017) Electrolytes for Li- and Na-ion batteries: concepts, candidates, and the role of nanotechnology. Elsevier Inc. https://doi.org/10.1016/B978-0-323-42977-1.00001-7
17. Quartarone E, Mustarelli P, Magistris A (1998) PEO-based composite polymer electrolytes. Solid State Ionics 110:1–14. https://doi.org/10.1016/s0167-2738(98)00114-3
18. Wang H, Sheng L, Yasin G, Wang L, Xu H, He X (2020) Reviewing the current status and development of polymer electrolytes for solid-state lithium batteries. Energy Storage Mater 33:188–215. https://doi.org/10.1016/j.ensm.2020.08.014
19. Fenton DE, Parker JM, Wright PV (1973) Complexes of alkali metal ions with poly(ethylene oxide). Polymer (Guildf) 14:589. https://doi.org/10.1016/0032-3861(73)90146-8
20. Ye L, Feng Z (2010) Polymer electrolytes as solid solvents and their applications. Polym Electrolytes Fundam Appl 550–582. https://doi.org/10.1533/9781845699772.2.550
21. Tarascon JM, Gozdz AS, Schmutz C, Shokoohi F, Warren PC (1996) Performance of Bellcore's plastic rechargeable Li-ion batteries. Solid State Ionics 86–88:49–54. https://doi.org/10.1016/0167-2738(96)00330-X
22. Ramesh S, Wen LC (2010) Investigation on the effects of addition of SiO2 nanoparticles on ionic conductivity, FTIR, and thermal properties of nanocomposite PMMA-LiCF3SO3-SiO2. Ionics (Kiel) 16:255–262. https://doi.org/10.1007/s11581-009-0388-3
23. Krawiec W, Scanlon LG, Fellner JP, Vaia RA, Vasudevan S, Giannelis EP (1995) Polymer nanocomposites: a new strategy for synthesizing solid electrolytes for rechargeable lithium batteries. J Power Sources 54:310–315. https://doi.org/10.1016/0378-7753(94)02090-P
24. Yue L, Ma J, Zhang J, Zhao J, Dong S, Liu Z, Cui G, Chen L (2016) All solid-state polymer electrolytes for high-performance lithium ion batteries. Energy Storage Mater 5:139–164. https://doi.org/10.1016/j.ensm.2016.07.003
25. Wieczorek W, Raducha D, Zalewska A, Stevens JR (1998) Effect of salt concentration on the conductivity of PEO-based composite polymeric electrolytes. J Phys Chem B 102:8725–8731. https://doi.org/10.1021/jp982403f
26 Wang W, Alexandridis P (2016) Composite polymer electrolytes: nanoparticles affect structure and properties. Polymers (Basel). 8:387. https://doi.org/10.3390/polym8110387
27. Hallinan DT, Balsara NP (2013) Polymer electrolytes. Annu Rev Mater Res 43:503–525. https://doi.org/10.1146/annurev-matsci-071312-121705
28. Gupta H, Singh SK, Singh VK, Tripathi AK, Srivastava N, Tiwari RK, Mishra R, Meghnani D, Singh RK (2019) Development of polymer electrolyte and cathode material for Li-batteries. J Electrochem Soc 166:A5187–A5192. https://doi.org/10.1149/2.0331903jes
29. Berthier C, Gorecki W, Minier M, Armand MB, Chabagno JM, Rigaud P (1983) Microscopic investigation of ionic conductivity in alkali metal salts-poly(ethylene oxide) adducts. Solid State Ionics 11:91–95. https://doi.org/10.1016/0167-2738(83)90068-1
30. Long L, Wang S, Xiao M, Meng Y (2016) Polymer electrolytes for lithium polymer batteries. J Mater Chem A 4:10038–10039. https://doi.org/10.1039/c6ta02621d
31. Singh SK, Shalu L, Balo H, Gupta VK, Singh AK, Tripathi YL, Verma RK (2018) Singh, Improved electrochemical performance of EMIMFSI ionic liquid based gel polymer electrolyte with temperature for rechargeable lithium battery. Energy 150:890–900. https://doi.org/10.1016/j.energy.2018.03.024
32. Choo Y, Halat DM, Villaluenga I, Timachova K, Balsara NP (2020) Diffusion and migration in polymer electrolytes. Prog Polym Sci 103:101220. https://doi.org/10.1016/j.progpolymsci.2020.101220
33. Wu X, Chen K, Yao Z, Hu J, Huang M, Meng J, Ma S, Wu T, Cui Y, Li C (2021) Metal organic framework reinforced polymer electrolyte with high cation transference number to enable dendrite-free solid state Li metal conversion batteries. J Power Sources 501:229946. https://doi.org/10.1016/j.jpowsour.2021.229946
34. Gorecki W, Andreani R, Berthier C, Armand M, Mali M, Roos J, Brinkmann D (1986) NMR, DSC, and conductivity study of a poly(ethylene oxide) complex electrolyte: PEO(LiClO4)x. Solid State Ionics 18–19:295–299. https://doi.org/10.1016/0167-2738(86)90130-X
35. Gorecki W, Jeannin M, Belorizky E, Roux C, Armand M (1995) Physical properties of solid polymer electrolyte PEO(LiTFSI) complexes. J Phys Condens Matter 7:6823–6832. https://doi.org/10.1088/0953-8984/7/34/007
36. Li X, Wang Z, Lin H, Liu Y, Min Y, Pan F (2019) Composite electrolytes of pyrrolidone-derivatives-PEO enable to enhance performance of all solid state lithium-ion batteries. Electrochim Acta 293:25–29. https://doi.org/10.1016/j.electacta.2018.10.023
37. Liu D, Purewal JJ, Yang J, Sudik A, Maurer S, Mueller U, Ni J, Siegel DJ (2012) MOF-5 composites exhibiting improved thermal conductivity. Int J Hydrogen Energy 37:6109–6117. https://doi.org/10.1016/j.ijhydene.2011.12.129
38. Polu AR, Rhee HW, Jeevan Kumar Reddy M, Shanmugharaj AM, Ryu SH, Kim DK (2017) Effect of POSS-PEG hybrid nanoparticles on cycling performance of polyether-LiDFOB based solid polymer electrolytes for all solid-state Li-ion battery applications. J. Ind. Eng. Chem. 45:68–77. https://doi.org/10.1016/j.jiec.2016.09.004
39. Xue Z, He D, Xie X (2015) Poly(ethylene oxide)-based electrolytes for lithium-ion batteries. J Mater Chem A 3:19218–19253. https://doi.org/10.1039/c5ta03471j
40. Gadjourova Z, Andreev YG, Tunstall DP, Bruce PG (2001) Ionic conductivity in crystalline polymer electrolytes. Nature 412:520–523. https://doi.org/10.1038/35087538
41. Shin JH, Henderson WA, Passerini S (2003) Ionic liquids to the rescue? Overcoming the ionic conductivity limitations of polymer electrolytes. Electrochem Commun 5:1016–1020. https://doi.org/10.1016/j.elecom.2003.09.017
42. Wang X, Zhai H, Qie B, Cheng Q, Li A, Borovilas J, Xu B, Shi C, Jin T, Liao X, Li Y, He X, Du S, Fu Y, Dontigny M, Zaghib K, Yang Y (2019) Rechargeable solid-state lithium metal batteries with vertically aligned ceramic nanoparticle/polymer composite electrolyte. Nano Energy 60:205–212. https://doi.org/10.1016/j.nanoen.2019.03.051
43. Zhou Q, Ma J, Dong S, Li X, Cui G (2019) Intermolecular chemistry in solid polymer electrolytes for high-energy-density lithium batteries. Adv Mater 31:1–21. https://doi.org/10.1002/adma.201902029
44. Xu Z, Yang T, Chu X, Su H, Wang Z, Chen N, Gu B, Zhang H, Deng W, Zhang H, Yang W (2020) Strong Lewis acid-base and weak hydrogen bond synergistically enhancing ionic conductivity of poly(ethylene oxide)@SiO2 electrolytes for a high rate capability Li-metal battery. ACS Appl Mater Interfaces 12:10341–10349. https://doi.org/10.1021/acsami.9b20128
45. Dirican M, Yan C, Zhu P, Zhang X (2019) Composite solid electrolytes for all-solid-state lithium batteries. Mater Sci Eng R Rep 136:27–46. https://doi.org/10.1016/j.mser.2018.10.004
46. Wang S, McGuirk CM, d'Aquino A, Mason JA, Mirkin CA (2018) Metal–organic framework nanoparticles. Adv Mater 30:1–14. https://doi.org/10.1002/adma.201800202
47. Liang F, Wen Z (2021) MOF/Poly(Ethylene Oxide) Composite polymer electrolyte for solid-state lithium battery. Wuji Cailiao Xuebao/J Inorg Mater 36:332–336. https://doi.org/10.15541/jim20200206
48. Choi JS, Son WJ, Kim J, Ahn WS (2008) Metal-organic framework MOF-5 prepared by microwave heating: factors to be

considered. Microporous Mesoporous Mater 116:727–731. https://doi.org/10.1016/j.micromeso.2008.04.033
49. Zhang Z, Huang Y, Gao H, Li C, Hang J, Liu P (2021) MOF-derived multifunctional filler reinforced polymer electrolyte for solid-state lithium batteries. J Energy Chem 60:259–271. https://doi.org/10.1016/j.jechem.2021.01.013
50. Moosavi SM, Nandy A, Jablonka KM, Ongari D, Janet JP, Boyd PG, Lee Y, Smit B, Kulik HJ (2020) Understanding the diversity of the metal-organic framework ecosystem. Nat Commun 11:1–10. https://doi.org/10.1038/s41467-020-17755-8
51. Kong L, Zhong M, Shuang W, Xu Y, Bu XH (2020) Electrochemically active sites inside crystalline porous materials for energy storage and conversion. Chem Soc Rev 49:2378–2407. https://doi.org/10.1039/c9cs00880b
52. Burgaz E, Erciyes A, Andac M, Andac O (2019) Synthesis and characterization of nano-sized metal organic framework-5 (MOF-5) by using consecutive combination of ultrasound and microwave irradiation methods. Inorganica Chim Acta 485:118–124. https://doi.org/10.1016/j.ica.2018.10.014
53. Kuppler RJ, Timmons DJ, Fang QR, Li JR, Makal TA, Young MD, Yuan D, Zhao D, Zhuang W, Zhou HC (2009) Potential applications of metal-organic frameworks. Coord Chem Rev 253:3042–3066. https://doi.org/10.1016/j.ccr.2009.05.019
54. Gerbaldi C, Nair JR, Kulandainathan MA, Kumar RS, Ferrara C, Mustarelli P, Stephan AM (2014) Innovative high performing metal organic framework (MOF)-laden nanocomposite polymer electrolytes for all-solid-state lithium batteries. J Mater Chem A 2:9948–9954. https://doi.org/10.1039/c4ta01856g
55. Angulakshmi N, Zhou Y, Suriyakumar S, Dhanalakshmi RB, Satishrajan M, Alwarappan S, Alkordi MH, Stephan AM (2020) Microporous metal-organic framework (MOF)-based composite polymer electrolyte (CPE) mitigating lithium dendrite formation in all-solid-state-lithium batteries. ACS Omega 5:7885–7894. https://doi.org/10.1021/acsomega.9b04133
56. Yuan C, Li J, Han P, Lai Y, Zhang Z, Liu J (2013) Enhanced electrochemical performance of poly(ethylene oxide) based composite polymer electrolyte by incorporation of nano-sized metal-organic framework. J Power Sources 240:653–658. https://doi.org/10.1016/j.jpowsour.2013.05.030
57. Yaghi OM, O'Keeffe M, Ockwig NW, Chae HK, Eddaoudi M, Kim J (2003) Reticular synthesis and the design of new materials. Nature 423:705–714. https://doi.org/10.1038/nature01650
58. Millward AR, Yaghi OM (2005) Metal–organic frameworks with exceptionally high capacity for storage of carbon dioxide at room temperature. J. Am. Chem. Soc. 127:17998–17999. https://doi.org/10.1021/JA0570032
59. Diddens D, Paillard E, Heuer A (2017) Improving the lithium ion transport in polymer electrolytes by functionalized ionic-liquid additives: simulations and modeling. J Electrochem Soc 164:E3225–E3231. https://doi.org/10.1149/2.0271711jes
60. Ebadi M, Costa LT, Araujo CM, Brandell D (2017) Modelling the polymer electrolyte/Li-metal interface by molecular dynamics simulations. Electrochim Acta 234:43–51. https://doi.org/10.1016/j.electacta.2017.03.030
61. Molinari N, Mailoa JP, Kozinsky B (2018) Effect of salt concentration on ion clustering and transport in polymer solid electrolytes: a molecular dynamics study of PEO-LiTFSI. Chem Mater 30:6298–6306. https://doi.org/10.1021/acs.chemmater.8b01955
62. Brooks DJ, Merinov BV, Goddard WA, Kozinsky B, Mailoa J (2018) Atomistic description of ionic diffusion in PEO-LiTFSI: effect of temperature, molecular weight, and ionic concentration. Macromolecules 51:8987–8995. https://doi.org/10.1021/acs.macromol.8b01753
63. Costa LT, Sun B, Jeschull F, Brandell D (2015) Polymer-ionic liquid ternary systems for Li-battery electrolytes: molecular dynamics studies of LiTFSI in a EMIm-TFSI and PEO blend. J Chem Phys 143:9. https://doi.org/10.1063/1.4926470
64. Singh VK, Shalu L, Balo H, Gupta SK, Singh RK (2017) Singh, Solid polymer electrolytes based on Li+/ionic liquid for lithium secondary batteries. J Solid State Electrochem 21:1713–1723. https://doi.org/10.1007/s10008-017-3529-z
65. Xue Y, Zheng S, Xue H, Pang H (2019) Metal-organic framework composites and their electrochemical applications. J Mater Chem A 7:7301–7327. https://doi.org/10.1039/C8TA12178H
66. Angulakshmi N, Kumar RS, Kulandainathan MA, Stephan AM (2014) Composite polymer electrolytes encompassing metal organic frame works: a new strategy for all-solid-state lithium batteries. J Phys Chem C 118:24240–24247. https://doi.org/10.1021/jp506464v
67. Angulakshmi N, Nahm KS, Nair JR, Gerbaldi C, Bongiovanni R, Penazzi N, Stephan AM (2013) Cycling profile of MgAl2O4-incorporated composite electrolytes composed of PEO and LiPF6 for lithium polymer batteries. Electrochim Acta 90:179–185. https://doi.org/10.1016/j.electacta.2012.12.003
68 Richard MN, Dahn JR (1999) Accelerating rate calorimetry study on the thermal stability of lithium intercalated graphite in electrolyte. II. Modeling the results and predicting differential scanning calorimeter curves. J Electrochem Soc 146:2078–2084. https://doi.org/10.1149/1.1391894
69. Richard MN, Dahn JR (1999) Accelerating rate calorimetry studies of the effect of binder type on the thermal stability of a lithiated mesocarbon microbead material in electrolyte. J Power Sources 83:71–74. https://doi.org/10.1016/S0378-7753(99)00260-8
70 Senthil Kumar R, Raja M, AnbuKulandainathan M, Manuel Stephan A (2014) Metal organic framework-laden composite polymer electrolytes for efficient and durable all-solid-state-lithium batteries. RSC Adv 4:26171–26175. https://doi.org/10.1039/C4RA03147D
71. Zhang Z, You JH, Zhang SJ, Wang CW, Zhou Y, Li JT, Huang L, Sun SG (2020) Metal organic framework nanorod doped solid polymer electrolyte with decreased crystallinity for high-performance all-solid-state lithium batteries. ChemElectroChem 7:1125–1134. https://doi.org/10.1002/celc.201901987
72. Dutta R, Kumar A (2016) Structural and dielectric properties of ionic liquid doped metal organic framework based polymer electrolyte nanocomposites. J Phys Conf Ser 765. https://doi.org/10.1088/1742-6596/765/1/012020
73. Qing X, Li J, Wang Z, Chen M, Lin J, Lin X (2020) A functionalized metal organic framework-laden nanoporous polymer electrolyte for exceptionally stable lithium electrodeposition. Chem Commun 56:15533–15536. https://doi.org/10.1039/d0cc06265k
74. Ataei F, Dorranian D, Motakef-Kazemi N (2021) Synthesis of MOF-5 nanostructures by laser ablation method in liquid and evaluation of its properties. J Mater Sci Mater Electron 32:3819–3833. https://doi.org/10.1007/s10854-020-05126-4
75. Sun H, Jin Z, Yang C, Akkermans RLC, Robertson SH, Spenley NA, Miller S, Todd SM (2016) COMPASS II: extended coverage for polymer and drug-like molecule databases. J Mol Model 22:1–10. https://doi.org/10.1007/s00894-016-2909-0
76 Peng Z, Ewig CS, Hwang MJ, Waldman M, Hagler AT (1997) Derivation of class II force fields. 4. Van der waals parameters of alkali metal cations and halide anions. J Phys Chem A 101:7243–7252. https://doi.org/10.1021/jp964080y
77. Ennari J (2008) Modelling of transport properties and state of water of polyelectrolytes containing various amounts of water. Polymer (Guildf) 49:2373–2380. https://doi.org/10.1016/j.polymer.2008.03.019
78. Zwanzig R (1961) Memory effects in irreversible thermodynamics. Phys Rev 124:983–992. https://doi.org/10.1103/PhysRev.124.983

79. Green MS (1952) Markoff random processes and the statistical mechanics of time-dependent phenomena. J Chem Phys 20:1281–1295. https://doi.org/10.1063/1.1700722
80 Kubo R (1957) Statistical mechanical theory of irreversible processes. I. General theory and simple applications to magnetic and conduction problems. J Phys Soc Japan 12:570–586. https://doi.org/10.1143/JPSJ.12.570
81. Srinophakun T, Martkumchan S (2012) Ionic conductivity in a chitosan membrane for a PEM fuel cell using molecular dynamics simulation. Carbohydr Polym 88:194–200. https://doi.org/10.1016/j.carbpol.2011.11.094
82. Pozuelo J, Riande E, Saiz E, Compañ V (2006) Molecular dynamics simulations of proton conduction in sulfonated poly(phenyl sulfone)s. Macromolecules 39:8862–8866. https://doi.org/10.1021/ma062070h
83 Wood WW, Parker FR (1957) Monte Carlo equation of state of molecules interacting with the Lennard-Jones potential. I. A supercritical isotherm at about twice the critical temperature. J Chem Phys 27:720–733. https://doi.org/10.1063/1.1743822
84. Brooks CL (1989) Computer simulation of liquids. J Solution Chem 18:99–99. https://doi.org/10.1007/BF00646086
85. Wang Z, Zhou H, Meng C, Xiong W, Cai Y, Hu P, Pang H, Yuan A (2020) Enhancing ion transport: function of ionic liquid decorated MOFs in polymer electrolytes for all-solid-state lithium batteries. ACS Appl Energy Mater 3:4265–4274. https://doi.org/10.1021/acsaem.9b02543
86. Scipioni R, Stixrude L, Desjarlais MP (2017) Electrical conductivity of SiO2 at extreme conditions and planetary dynamos. Proc Natl Acad Sci U S A 114:9009–9013. https://doi.org/10.1073/pnas.1704762114